Pulsars in the High Energy and Early Universe

John Middleditch[1], John Singleton[1], Andrea C. Schmidt[1],
Houshang Ardavan[2], Arzhang Ardavan[3]
([1]MPA-CMMS, Los Alamos National Lab., [2]IoA, Cambridge U., [3]Clarendon Lab., Oxford U.)

The mechanism of polarization currents excited supraluminally (updated faster than c) by rotating neutron star magnetospheres (SLIP) can be used to explain the means by which supernova progenitors are disrupted, including the details of SN 1987A. At radii of a few times that of the light cylinder the effect helps to lift material way from the core. At much larger radii, the paths from current-containing annuli clear the stellar core on the way to the poles, where the concentration of the effects results in highly collimated pulsar-driven jets with velocities in excess of 0.95c, and element transmutation via the r-process. SLIP also accounts for the anomalous dimming of SNe Ia at cosmological distances, jets from Sco X-1 and SS 433, the lack/presence of pulsations from the high/low luminosity low mass X-ray binaries, long/short gamma-ray bursts, and predicts that their afterglows are the pulsed optical-/near-infrared emission associated with the pulsars. Pulsar-driven jets from the SNe of the first stars may allow galaxies to form without the need for dark matter. SLIP may also account for the TeV e+/e- results from PAMELA and ATIC, the WMAP "haze"/Fermi "bubbles", and the spectrum of the nine Fermi-LAT pulsars with radio observations, over 16-18 orders of magnitude of frequency with minimal adjustable parameters. With parameters extracted from the broadband fits, we have calculated values for the number density of electrons and the magnetic field, B, at the emitting region and derived some systematic properties of these pulsars' plasma atmospheres.

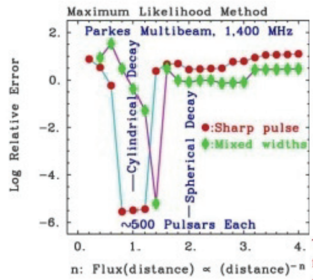

Fig. 3. The method of Efstathiou et al. (1988) as applied by Singleton et al. [arXiv:0912.0350] shows that those pulsars in the Parkes Multibeam Survey with sharp pulses (full width half maxima <3% of their periods) dim only as 1/distance, while those with wider pulses are displaced toward distance^{-2} as predicted by SLIP.

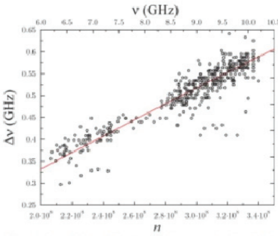

The predicted oscillations of the spectrum of the emission for w/(2p) = 30.3 Hz and W/w ~ 1.9 x 104, have the same spacing as those of the emission bands in the observed spectrum of the Crab pulsar (Hankins & Eilek 2007).

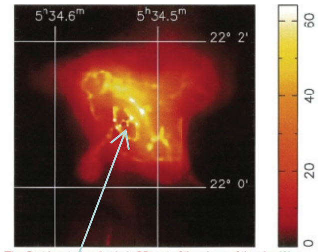

The Crab's rotational axis is 25° out of the plane of the sky. We observe the interpulse well away from the favored direction for plasma just outside the light cylinder (~equatorial). Thus its pulse profile is similar to the green upper curve, confirming SLIP again.

$$\frac{dP_n}{d\Omega_P} \propto S_1(n)^2 \mathrm{Ai}^2\left[-\left(\frac{2}{n}\right)^{1/3}\frac{\Omega}{\omega}\right] + S_2(n)^2\left(\frac{2}{n}\right)^{2/3}\mathrm{Ai}'^2\left[-\left(\frac{2}{n}\right)^{1/3}\frac{\Omega}{\omega}\right] + 2S_3(n)^2\left(\frac{2}{n}\right)^{1/3}\mathrm{Ai}\left[-\left(\frac{2}{n}\right)^{1/3}\frac{\Omega}{\omega}\right] \times \mathrm{Ai}'\left[-\left(\frac{2}{n}\right)^{1/3}\frac{\Omega}{\omega}\right], \quad (4)$$

in which

$$S_1(n) = n^{2/3}|K_r||K_{\varphi 0}|\left(|\bar{s}_r|^2 + |\bar{s}_\varphi \cos\theta_P - \bar{s}_z \sin\theta_P|^2\right)^{1/2},$$
$$S_2(n) = n^{2/3}|K_r||K_{\varphi 0}|\left(|\bar{s}_\varphi|^2 + |\bar{s}_r|^2\cos^2\theta_P\right)^{1/2},$$

and

$$S_3(n) = n^{2/3}|K_r||K_{\varphi 0}| \times \left\{\Im\left[\bar{s}_r^* \cos\theta_P(\bar{s}_\varphi\cos\theta_P - \bar{s}_z\sin\theta_P) - \bar{s}_r\bar{s}_\varphi^*\right]\right\}^{1/2}.$$

The power radiated per harmonic per solid angle. Here, $s_{r,\varphi,z}$ are the Fourier components of the source densities $s_{r,\varphi,z}$ $l_{m\cos\theta_P}$ wrt z. $\Im$ and * denote imaginary part and complex conjugate, and $(R_P, \theta_P, \varphi_P)$ are the spherical polar coord. of the observation point, P. $K_{\varphi 0}$ is defined by:

$$K_{\varphi 0} = (-1)^{n+m}\sin\left(\frac{\pi\Omega}{\omega}\right)\left(\frac{\mu_+}{n-\mu_+} + \frac{\mu_-}{n-\mu_-}\right),$$

and the various frequencies involved (n, m, etc.) are tabulated in the upper right.

Frequency	Definition
$\frac{\omega}{2\pi}$	pulsar rotation frequency
$\nu = \frac{n\omega}{2\pi}$	observation frequency
$\frac{m\omega}{2\pi}$	azimuthal modulation frequency
$\frac{\Omega}{2\pi}$	temporal modulation frequency
μ_+	$\frac{\Omega}{\omega} + m$
μ_-	$\frac{\Omega}{\omega} - m$

Function	Frequency range	Limiting value
$\mathrm{Ai}\left[-\left(\frac{2}{n}\right)^{1/3}\frac{\Omega}{\omega}\right]$	$n \ll \left(\frac{\Omega}{\omega}\right)^3$	$\left(\frac{2}{n}\right)^{-\frac{1}{12}}\left(\frac{\Omega}{\omega}\right)^{-\frac{1}{4}}$
$\mathrm{Ai}\left[-\left(\frac{2}{n}\right)^{1/3}\frac{\Omega}{\omega}\right]$	$n \gg \left(\frac{\Omega}{\omega}\right)^3$	Ai(0)
$\mathrm{Ai}'\left[-\left(\frac{2}{n}\right)^{1/3}\frac{\Omega}{\omega}\right]$	$n \ll \left(\frac{\Omega}{\omega}\right)^3$	$\left(\frac{2}{n}\right)^{\frac{1}{12}}\left(\frac{\Omega}{\omega}\right)^{\frac{1}{4}}$
$\mathrm{Ai}'\left[-\left(\frac{2}{n}\right)^{1/3}\frac{\Omega}{\omega}\right]$	$n \gg \left(\frac{\Omega}{\omega}\right)^3$	Ai'(0)
$K_{\varphi 0}$	$n \ll \mu_+$	~ 1
$K_{\varphi 0}$	$n \sim m \gg \frac{\Omega}{\omega}$	$\sim n$
$K_{\varphi 0}$	$n \gg \mu_+$	$\sim n^{-1}$
K_r	$n \ll \frac{\pi R_P}{(\hat{r}_> - \hat{r}_<)^2}$	$\simeq \hat{r}_> - \hat{r}_<$
K_r	$n \gg \frac{\pi R_P}{(\hat{r}_> - \hat{r}_<)^2}$	$\simeq \left(\frac{2\pi}{n}R_P\right)^{\frac{1}{2}}\exp\left(-\frac{i\pi}{4}\right)$

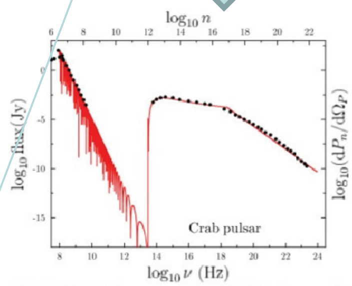

The SLIP fit to the observational data of the Crab pulsar over 16 orders of magnitude. The curves show the log($dP_n/d\Omega_P$) vs. log n and log ν, for $\nu = n\omega/(2\pi) \sim 30.3n$ Hz and $\Omega/\omega \sim 1.9 \times 10^4$. The UV recovery (~$10^{15}$ Hz) is due to the az. mod. Freq. $m\omega/(2\pi) \sim 3 \times 10^{13}$ Hz. The Rayleigh distance makes the 10^{18} Hz break.

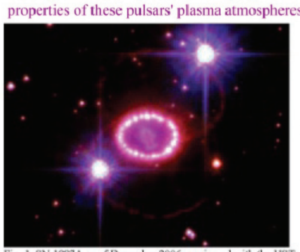

Fig. 1. SN 1987A as of December 2006, as viewed with the HST (NASA, P. Challis, & R. Kirshner, Harvard-Smithsonian Center for Astrophysics). North is up, east is to the left. The axis of the bipolarity corresponds to the "Mystery Spot" bearing of 194° (the far-side [southern] minor axis of the equatorial ring has a bearing of 179°). The pulsar within this remnant (and all other remnants as well) caused this bipolarity (see further below).

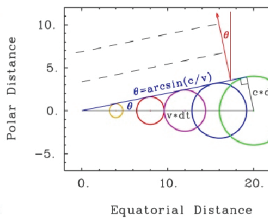

Huygens' wavelets of a supraluminal disturbance (v=5c) propagating from right to left form two fronts, each with a polar angle of arcsin(v/c). Emission in these directions (two circles on the sky) decays only as 1/distance.

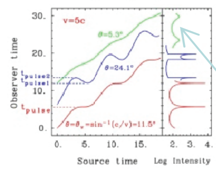

For the lower curve, a time source of finite dimension (1) contributes to a single time (dimension 0) for an observer. Thus the intensity of the pulsations, in the direction represented by this curve (the "cusp" -- polar angle θ_v) only as 1/distance, and this goes on *forever* for the cusp – the further away the observer, the more source contributes to the signal. For observers at larger polar angles, as for the middle curve, two still narrow peaks are observed in the pulse profile, and the intensity drops with the usual 1/distance^2 law. At smaller polar angles (top curve), the pulse profile consists of only a broad, weak, single peak.

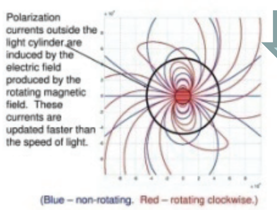

(Blue – non-rotating. Red – rotating clockwise.)

Fig. 4. A rotating, magnetized body produces a periodic disturbance, even beyond its light cylinder, which, if there is plasma available, induces polarization currents that are updated at a rate faster than the speed of light.

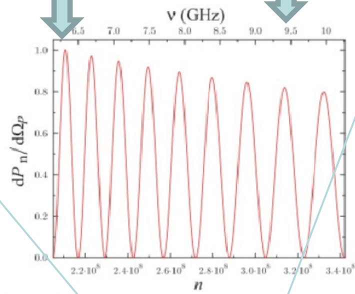

The predicted oscillations of the spectrum of SLIP emission for ω/(2π) = 30.3 Hz and Ω/ω ~ 1.9 x 10^4. The actual spectrum shown below is identical to this.

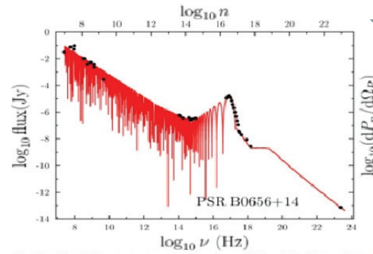

Another Fermi Gamma-ray pulsar for $\nu = n\omega/(2\pi) \sim 2.6n$ Hz, and $\Omega/\omega \sim 5.89 \times 10^5$. The resonant enhancement due to the aximuthal frequency $m\omega/(2\pi) \sim 5.2 \times 10^{14}$ Hz. The steepening in the gradient of the spectrum by -1 at 1.8 x 10^{19} Hz corresponds to crossing the Rayleigh distance. Vela, Geminga, B1055-52, B1509-58, B1706-44, B1929+10, and B1951+32 fits were also successful.

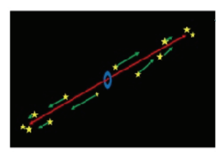

Do the jets from the pulsars produced by the 1st SNe allow the formation of galaxies within 500 million years? Maybe! They do trash a lot of entropy between stars. They inhibit star formation locally, but space is vast, and the pulsar-driven plumes (aka "Mystery Spot"), in addition to inducing star formation in lines along their paths, may plough up enough material to form stars at their endpoints.

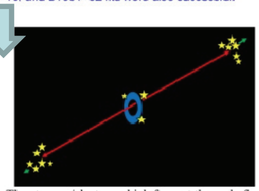

The streams/clusters which form at the end of the jets retain a small fraction of the initial jet velocity (~0.2 c), which may explain the results from GALEX, where near pairs of distant galaxies have velocities which do not reflect their mutual gravitational attraction.

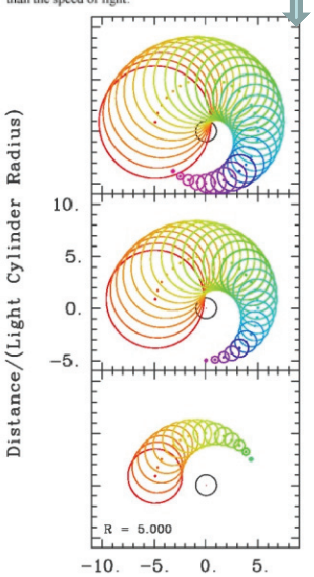

Huygen's wavelets for a polarization current source rotating counterclockwise at 5 times the light cylinder radius (v=5c), starting at 9:10 o'clock (bottom frame, left largest red circle), and ending at 7 o'clock (top frame, magenta dot), produce a pattern of emission which is initially focused (a "cusp") on its light cylinder (inner black circle) at 11:30 o'clock (middle frame), and then progresses to 12:30 o'clock (and eventually out of the plane with time at a polar angle of arcsin (c/v)). The range of sources (dots), contributing to the cusp, runs from red into green and eventually into blue (9:10 o'clock to 3 o'clock). This is a rotation-powered pulsar. If v=100c (plasma at 100 light cylinder radii), this is a supernova. If you get in front of this, you, and a lot of starguts, will end up going very, very fast.

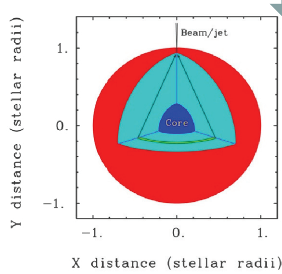

Annuli with radii larger than the stellar core radius (green) have a relatively unimpeded influence on the rest of the star, including the poles, where the timing relation (and decay only as 1/distance) drives strong, highly collimated polar beams and jets.

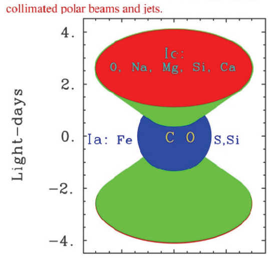

The pulsar remnant in SNe Ia/c transmutes elements through the r-process while driving these (Na, Mg, Ca) in polar jets, even in or near the stellar photosphere. This happens because carbon and oxygen are available there (as they are throughout the rest of the progenitor). SLIP is the only SN model which accounts for the lines of r-process elements observed even in very early spectra of SNe Ic.

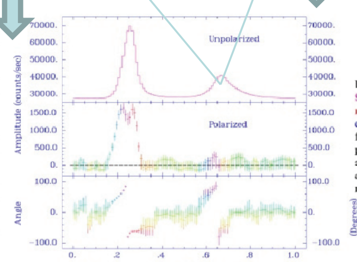

(Top) The optical pulse profile of the Crab Pulsar. (Middle) The polarized pulse profile. (Bottom) The polarization angle of the pulse profile. The spectrum of a giant radio interpulse sub-pulse shows the bands predicted by SLIP (see below).

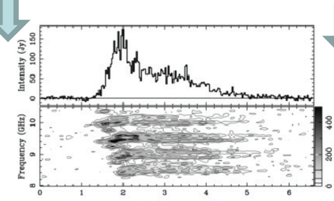

A radio spectrum of a typical giant interpulse, from Hankins & Eilek 2007, shows the bands predicted by SLIP. Giant pulses in the main peak do not show these bands, thus the Crab's pulse and interpulse have different origins. The interpulse is consistent with a view closer to the rotational axis than the optimum angle given by arcsin(c/v), as given by the upper pulse profile of the three shown in a previous frame, and the orientation given by the Crab pulsar movie of Hester et al., 2002, shown in another frame to follow.

Conclusions

The model of pulsar emission by supraluminally induced polarization currents (SLIP) provides a means by which spinning neutron stars can disrupt their progenitor stars and drive highly collimated polar beams and relativistic jets. These can account for SN 1987A's beam, jet, and "Mystery Spot," the bipolarity of all other SNe, the jets of Sco X-1 and SS 433, the multi-GeV e$^+$ excess, the r-process, and possibly star formation in the early Universe without dark matter. In particular, SLIP accounts for the spectra of 9 broad-band pulsars over their entire known spectrum. SLIP also predicts that gamma-ray burst afterglows will be pulsars, which enforce a toroidal geometry on the equatorial ejecta of supernovae. This geometry and mechanism apply to all SNe observed so far, which makes it extraordinarily difficult to calculate, or to establish a representative local sample of any type of SNe, including Ia's. Because local SNe Ia's were selected on the basis of obeying the width-luminosity relation, in which the e$^+$e$^-$ γ-rays were well encapsulated, this sample must lie at the high end of the range in mass, and hence is too luminous to be representative of a distant sample which could not be so carefully selected. The most likely interpretation of SNe Ia data is that there is no anomalous dimming of the distant sample, and therefore ***no direct evidence at all for the existence of dark energy***. This work was supported in part by Los Alamos National Laboratory LDRD grants 20080085DR and 20110320ER.